Heterologous Expression and Characterization of *ToxA1* haplotype from India and its interaction with *Tsn1* for Spot Blotch Susceptibility in spring wheat

Ranjan Kumar Chaubey[1], Dharamsheela Thakur[2], Sudhir Navathe[3*], Sandeep Sharma[1], Vinod Kumar Mishra[1], Pawan Kumar Singh[4]*, Ramesh Chand*

[1] Institute of Agricultural Sciences, Banaras Hindu University Varanasi 221005, India

[2] Department of Molecular Biology and Genetic Engineering, Bihar Agricultural University, Sabour 813210, Bhagalpur, India;

[3] Agharkar Research Institute, G. G. Agarkar Road, Pune 411004, India

[4] International Maize and Wheat Improvement Center (CIMMYT), Texcoco 56237, Mexico.

* Correspondence:

Ramesh Chand, Banaras Hindu University, Varanasi, India, Email: rc_vns@yahoo.co.in;

Sudhir Navathe, Agharkar Research Institute, Pune, India, Email: snavathe@aripune.org

Abstract

ToxA a necrotrophic effector protein, is known to be present in the genome of fungal species like *Parastagnospora nodorum*, *Pyrenophora tritici-repentis* and *Bipolaris sorokiniana. Tsn1* is the sensitivity gene in the host whose presence indicates more susceptibility to *ToxA* carrying pathogen, and *ToxA-Tsn1* delivers an inverse gene-for-gene relationship. The present study involved cloning and expressing the *ToxA1* gene from *B. sorokiniana*. It was found that the amplicon exhibited an expected product size of 471 bp. Sequence analysis of the *ToxA1* nucleotide sequence revealed the highest identity, 99.79%, with *Py. tritici-repentis*. The protein expression analysis showed peak expression at 16.5kDa. Phylogenetic analysis of *ToxA1* sequence from all the *Bipolaris* isolates formed independent clade along with *Py. tritici-repentis* and diverged from *P. nodorum*. *ToxA-Tsn1* interaction was studied in 18 wheat genotypes (11 *Tsn1* and 7 *tsn1*) at both the seedling and adult stage, validating the inverse gene-for-gene relationship, as the toxin activity was highest in the K68 genotype (*Tsn1*) and lowest in WAMI280 (*tsn1*). This shows a path towards more genomic regions involved in resistance to spot blotch disease, which could be further explored.

Keywords: *Bipolaris sorokiniana*, effector-triggered susceptibility, the inverse gene for gene relationship, sensitivity genes, *ToxA1*, *Triticum aestivum*

Introduction

Host selective toxins (HSTs) are the effector molecule released during the invasion of necrotrophic pathogens and act as major determinants of pathogenicity (Ciuffetti et al. 1997). These necrotrophic effectors are specific biomolecules that are structurally complex, chemically diverse, and responsible for causing some key diseases in important crops. HSTs are very important in host-pathogen interaction but are produced by limited genera of fungi involving multiple toxins (Wolpert et al. 2002). Spot blotch of wheat is a threatening disease caused by *Bipolaris sorokiniana*, a hemi-biotrophic pathogen. This disease is mainly prevalent in South Asia's warm, humid region, especially in the eastern Indo-Gangetic plains of India. Wheat productivity can decline by 40% due to spot blotch alone (Sharma et al. 2006). Spot blotch has been reported to cause up to 17.5% yield loss in the Indian sub-continent, and about 25mha of wheat is affected by spot blotch worldwide (Pandey et al. 2021). Plant pathogens have their genetic makeup for causing host infection, which is decided by the presence of a single gene that confers host susceptibility or resistance (Balance et al. 1989, Friesen et al. 2006). The proteinaceous necrotrophic effector ToxA a major HST produced by *B. sorokininana*. Apart from this, ToxA is known to be produced from two necrotrophic pathogens, *P. nodorum* and *Py. tritici-repentis* and cause *Parastagnospora* nodorum blotch and tan spot, respectively (Solomon et al. 2006, Tuori et al. 1995). ToxA protein was originally reported in a culture filtrate of the wheat pathogen *Py. tritici-repentis* (Tuori et al. 1995). The ToxA protein was first discovered by Tomás and Bockus (1987) from the culture filtrate of *Py. tritici-repentis*. The *ToxA* manifested high nucleotide diversity in *S. nodorum,* whereas it showed a lack of variation in *Py. tritici-repentis*. This pattern of nucleotide diversity and the recent emergence of tan spot suggests the recent introduction of *ToxA* into *Py. tritici- repentis* genome (Friesen et al. 2006). The *ToxA* sequences from *S. nodorum* and *Py. tritici-repentis*

depicted differences at four fixed nucleotide sites resulting in two predicted amino acid changes consistent with the interspecific transfer of this gene from *S. nodorum* into *Py. tritici-repentis* (Friesen et al. 2006), and this *ToxA* gene jumped horizontally from *Py. tritici-repentis* to *B. sorokiniana,* (McDonald et al. 2018). *ToxA* and its surrounding 14 kb suggest that this gene was horizontally transferred, facilitated by a type II DNA transposon (McDonald et al. 2019). *ToxA* is a single-copy gene, and it was found to be embedded within a 12-kb genomic element nearly identical to the corresponding regions in *P. nodorum* and *Py. tritici-repentis* (McDonald et al. 2018). The mature ToxA protein is 13.2 kDa, and it encodes a signal peptide of 23 amino acids and a pro-domain of 4.3kDa (required for protein folding), and both are cleaved before the secretion of mature ToxA protein (Balance at al. 1996, Ciuffetti et al. 1997, Tuori et al. 2000). Studies revealed that the host sensitivity of ToxA was mapped on wheat chromosome arm 5BL, and the sensitivity gene was named *Tsn1* (Faris et al. 2010). Further, it was confirmed that this gene was significant for both tan spot and SNB, and in both cases, the pathogen had a sensitivity gene such as *ToxA* (Lamari and Bernier 1989, Friesen et al. 2006). It is considering the wheat-*B. sorokiniana* pathosystem, *ToxA* confers virulence, and it is the only known virulence gene whose corresponding sensitivity gene (*Tsn1*) in the host is identified. Further, it was also demonstrated that *Tsn1*-carrying wheat cultivars are more sensitive to *B. sorokiniana* isolates that harboured the *ToxA* gene. Cloning of the *Tsn1* gene unfolded characteristics similar to classical disease resistance nucleotide-binding leucine-rich repeat NLR gene that included serine/threonine kinase, leucine-rich repeats, nucleotide binding and protein kinase domains (Faris et al. 2010). The ToxA gene is transcribed as a necrotrophic effector protein responsible for infection in the host, with *Tsn1* being a resistance gene (Tan et al. 2016). A resistance-like gene *Tsn1* in wheat is responsible for conferring susceptibility to *ToxA* in *Py. tritici-repentis* and *P. nodorum* isolates (Friesen et al. 2006). This *ToxA–Tsn1* interaction system has been proved as an example of the inverse gene-for-gene relationship. It

99 was realizing the occurrence of spot blotch in South Asia and the emergence of *ToxA1* as a key
100 virulence gene driven us towards studying this host-pathogen relation. Keeping this in mind,
101 we cloned the *ToxA1* gene from *B. sorokiniana* and conducted expression analysis for the
102 ToxA1 protein. We also validated the pathogenicity of *ToxA1* on the allelic status of *Tsn1* by
103 using 18 *Tsn1/tsn1* genotypes.

104 **Materials and Methods**

105 ***Primer designing:***

106 The *ToxA* sequence from *Py. tritici-repentis* (U79662.1) was obtained in FASTA format from
107 NCBI (National Centre for Biotechnology Information) GenBank database
108 (https://www.ncbi.nlm.nih.gov/genbank/). *ToxA* is a 534bp-long gene sequence, and primers
109 were designed using the web-based tool Primer-BLAST (Basic Local Alignment Search Tool)
110 from NCBI. The primers were utilized to amplify *ToxA1* in *B. sorokiniana* isolate MCC 1533
111 (Pusa2). The isolate MCC1533 (Pusa 2) has been identified and deposited at National Center
112 for Microbial Resources (NCMR), Pune, India. The primer sequence used is given as Forward
113 Primer (FP) -CGCGGATCCGATCCCGGTTACGAAATCG and Reverse Primer (RP) - CGC
114 CTCGAGCTAATTTTCTAGCTGCATTCTC

115 ***RNA extraction and cDNA synthesis***

116 *B. sorokiniana* isolate MCC 1533 (Pusa2) was cultured for 10 days in a Potato Dextrose Broth.
117 Mycelium was harvested, and the total RNA was isolated using Invitrogen PureLink^{TM} RNA
118 Mini kit following the manufacturer's protocol. The integrity and size distribution of total RNA
119 purified with RNeasy Kit was checked by 1.2% agarose gel electrophoresis and ethidium
120 bromide staining visualizing two sharp bands of 28S rRNA to 18S RNA. The nanodrop results
121 were obtained with the Nanodrop2000 instrument (Thermo Scientific), which showed the
122 acceptable purity of RNA isolated from each biological replicate (A_{260}/A_{280} of 1.9 to 2.1). The
123 isolated RNA was stored immediately at -80°Cin nuclease-free water (supplied with the kit)

124 for further analysis. cDNA was synthesized using a Thermo cDNA synthesis kit following the
125 manufacturer's protocol.
126 RNA previously isolated from the biological sample was taken as a template for cDNA
127 synthesis. An additional treatment of RT enhancer was included during cDNA synthesis as
128 supplied and instructed with the kit and manufacturer's protocol to prevent chances of
129 contamination of genomic DNA during isolation. The template RNA sample was added to the
130 cDNA reaction mixture, which was obtained by diluting the biological samples of RNA.
131 ***ToxA gene cloning***
132 The expression constructs were produced in the bacterial expression vector pET28a that directs
133 the expression of HIS-tagged fusion proteins in *E. coli*. BamH1 and Xho restriction sites were
134 introduced in forward and reverse primer for cloning in PET vector. Primers were designed
135 such that the PCR amplified portion of the *ToxA* gene was generated with a 5' *Bam*HI site and
136 a 3' *Xho* site. The PCR products were digested with *Bam*HI and *Xho*, gel-purified with the
137 QIAquick Gel Extraction Kit (Qiagen, Valencia, CA) and cloned into the *Bam*HI and *XhoI*
138 sites of pET28a. Primers FP-CGCGGATCCGATCCCGGTTACGAAATCG and RP- CGC
139 CTCGAGCTAATTTTCTAGCTGCATTCTC were used for the PCR amplification. PCR
140 amplification was performed using cDNA as a template in an Eppendorf Mastercycler using
141 the following cycles; initial denaturation of 95°C for 7 min followed by 35 cycles of 94°C (30
142 s), 55°C (45 s) and 72°C (1 min) and a final extension of 10 min at 72°C. The PCR product
143 was gel-purified, digested with *Bam*HI and *XhoI*, and ligated into the respective restriction sites
144 of pET28a. The resulting construct contained the predicted effector protein gene fused to a 6X
145 histidine tag at the N-terminus. The ligated product was used to transform *E. coli* DH5alpha
146 and BL21 (DE3) strains (Sambrook et al. 2006) for cloning and protein expression.
147 ***Sequencing and characterization***

148 Cloned fragment of *ToxA1* from *B. sorokiniana* isolate MCC1533 (Pusa2) was sequenced by
149 Sanger sequencing. The sequences obtained in two frames were merged, and overlapping
150 sequences were identified in both directions using Bioedit Sequence Alignment Editor (Hall
151 1999). Merged sequences were then prepared in a single frame. The sequences have been
152 deposited to the National Centre for Biotechnology Information (NCBI) database with Gene
153 Bank accession number (OP289649). The processed *ToxA1* sequence was used as a query for
154 BLASTn (https://blast.ncbi.nlm.nih.gov/Blast.cgi) for finding homologous sequences with
155 reference to the NCBI nucleotide database (Altschul et al. 1997). The processed *ToxA1*
156 nucleotide sequence was then translated to the amino acid sequence in BioEdit 7.2. Sequences
157 of *Py. tritici-repentis, P. nodorum* and different isolates of *B. sorokiniana* were retrieved from
158 the NCBI protein database. The amino acid sequences retrieved using BLASTp searches were
159 then used to create Multiple sequence alignments of 27ToxA sequences. MEGA X (Molecular
160 Evolution Genetics Analysis) software (Kumar et al. 2018) was then used to create a phylogeny
161 of *ToxA* amino acid sequences of 49 isolates of *Py. tritici-repentis, P. nodorum* and *B.*
162 *sorokiniana* using the CLUSTAL W alignment algorithm (Larkin et al. 2007). All the
163 alignment settings were employed at default values; 178 and 114 positions with and without
164 gaps were obtained, respectively. The substitutions selected with complete deletion of gaps or
165 missing data were used to analyze sequences. The phylogenetic tree was inferred using the
166 maximum likelihood method based on the JTT model (Jones et al. 1992). The initial tree was
167 inferred with the default setting using the Neighbour Joining method, and Nearest-Neighbour
168 Interchange was used as an ML heuristic search method. The reconstructions of phylogenetic
169 trees were conducted using the Maximum Likelihood Method. Bootstrap with 1000 replicates
170 for the Poisson correction model was performed to assess node support (Felsenstein 1985).

171 ***Protein modelling and topographical properties***

172 The predicted protein sequence of cloned Pusa-2 *ToxA1* was subjected to the SWISS-MODEL
173 homology modelling online tool (Arnold et al. 2006). Proteins were modelled utilizing Protein
174 Data Bank (PDB) entry 1zld.1.A (*Py. tritici-repentis*) as reference. The quality of modelled
175 protein was judged based on GMQE (Global Model Quality Estimation) and QMEAN
176 (Qualitative Model Energy Analysis) Z-score parameters (Benkert et al. 2009, Studer et al.
177 2020). The best model was selected based on the GMQE score, which ranges from 0 to 1, with
178 a higher value indicating better reliability. The QMEAN Z-score estimates the "degree of
179 nativeness" of the structural features observed in the model on a global scale. QMEAN Z-
180 scores around zero indicate good agreement between the model structure and experimental
181 structures. Scores of -4.0 or below is an indication of models with low quality. The quality of
182 the resulting models was also monitored with PROCHECK and ProsSA-WEB (Laskowski et
183 al. 1993). Geometrical and topographical properties of the modelled proteins were identified
184 using the Computed Atlas of Surface Topography of proteins (CASTp) 3.0 online server (Tian
185 et al. 2018). Molecular graphics images were produced using the UCSF Chimera package
186 (Pettersen et al. 2004). The alpha helix and the beta-sheet percentage were analyzed using
187 PDBMD2CD.

188 ***Isolation of proteins from E. coli cultures***

189 *E. coli* cultures harbouring all expression constructs were grown overnight in 5 ml of LB
190 (Sambrook et al. 2006) with 100µg of kanamycin per ml (LBA) at 37°C and shaking at 250
191 rpm (G24 Incubator Shaker, New Brunswick Scientific, Edison, NJ). Two hundred and fifty
192 microliters of the overnight culture were used to inoculate 25 ml of fresh LBA and incubated
193 with shaking at 37°C for 1 h. Expression of fusion proteins was induced by the addition of
194 isopropyl-beta-Dthiogalactopyranoside (IPTG) to a final concentration of 1 mM, and the
195 cultures were incubated for an additional 4hrs under the same conditions. Cells were harvested
196 by centrifugation at 4,000× *g,* 4°C for 20 min and the pellets were resuspended in cold

197 sonication buffer (SB; 50 mM Na2HPO4, 5 mM Tris-base, 300 mM NaCl, pH 8.0) with 0.5%
198 Triton-x-100 and 10 mM DTT. Resuspended pellets were sonicated three times, 30 s each, with
199 2 min on ice between periods. Insoluble material was then pelleted by centrifugation at 10,000
200 × *g,* 4°C, for 10 min. Pellets were washed thrice with SB with 0.5% Triton-× -100 and 10 mM
201 DTT. The final washed pellets, containing inclusion bodies, were either stored frozen at –80°C
202 or resuspended in 1 ml of 8 M guanidine HCl (Sigma) in refolding buffer (250 mM NaCl, 100
203 mM sodium phosphate buffer, 10 mM Tris-base, 4% glycerol, 1 mM EDTA, and 0.005 %
204 Tween 20, pH 8.0) with freshly prepared DTT added to a final concentration of 10 mM.
205 Solubilized proteins were sonicated briefly twice (for 5 to 10 s) and then heated to 37°C for 10
206 min and 50°C for an additional 5 min to assist in the solubilization of proteins. Insoluble
207 material was removed from the samples by centrifuging at 12,000 ×*g* for 10 min. Then,
208 solubilized proteins were quantitated with Bradford assay reagent (Bio-Rad, California, USA)
209 with bovine serum albumin used as a standard. Fusion proteins solubilized in guanidine HCl
210 were used immediately.

211 ***Screening of ToxA1 –Tsn1 interaction on different wheat genotypes***

212 The screening of 18 wheat genotypes was conducted for *Tsn1/tsn1,* out of which 11 genotypes
213 harbouring Tsn1 and the rest 7 genotypes with *tsn1* were sown in 3 replications at polyhouse,
214 Plant Pathology, Institute of Agricultural Sciences, Banaras Hindu University in 1m rows at a
215 distance of 22.5cm. Infiltration of ToxA1 protein, as well as control (Uninduced protein), was
216 done at both the seedling stage (3-5 leaf stage) and adult stage (Zadoks 55). 250µg of ToxA
217 protein was infiltrated by a sterilized syringe, and symptoms were recorded 7 days after
218 infiltration. Photographic data was captured using a Nikon camera. The size of the lesion was
219 measured using ImageJ software.

220 ***Statistical Analysis***

221 The lesion size was measured in length, width, and area of lesions. The statistical analysis was
222 conducted for phenotypic traits, including length, width, and area of necrotic lesions of wheat
223 genotypes with the *Tsn/tsn1* gene at both seedling and adult stages. The correction coefficients
224 between disease components were calculated using R software V 4.2.1 (R Core Team, 2022).
225

226 **Results**

227 ***Cloning and Expression study of ToxA1***

228 The *ToxA* gene from *B. sorokiniana* was amplified using primers designed from *PtrToxA*
229 through RT-PCR. The amplicon exhibited the expected product size of 471bp, which was then
230 cloned in the pET28avector. The cloned gene was validated using colony PCR of the
231 transformed cell. The *ToxA1* gene, after validation, was subjected to sequencing, and the
232 sequence data after processing revealed successful cloning of the *ToxA* gene (now *ToxA1- B.*
233 *sorokininana*). This ToxA1 nucleotide sequence was further used for BLASTn analysis,
234 revealing the highest identity, 99.79%, with *Py. tritici-repents* and E-value close to zero. The
235 cloned gene was then subjected to their expression at different concentrations of IPTG, namely,
236 at 0.4mM, 0.6mM, 0.8mM and 1.0mM, and expression of the *ToxA1* gene was highest at
237 1.0mM concentration with an expected band size of 16.5kDa in sodium dodecyl sulfate (SDS)-
238 polyacrylamide gels (Fig. 1).

239 ***ToxA1 characterisation and Phylogenetic analysis***

240 The identification of *ToxA1* after showing sequence similarity with *Py. Tritici-repentis* ToxA
241 using BLASTn analysis on NCBI was conducted. Further characterisation of ToxA1 was
242 conducted by translating the nucleotide sequence to amino acid sequence using the web-based
243 tool Expasy (https://www.expasy.org/resources/translate). The amino acid sequence of ToxA1
244 was subjected to BLASTp analysis on NCBI, which depicted 100% similarity with *Py. tritici-*
245 *repentis* showing E value 9e-109. Multiple sequence alignment of 25ToxA protein sequences

246 and *ToxA1* MCC1533 (Pusa2) translated sequence in Bioedit revealed that amino acid
247 differences were found in most *P. nodorum* strains. However, the cloned Pusa2_*ToxA1*
248 sequence showed complete similarity to *Py. tritici-repentis*. *P. nodorum* depicted amino acid
249 substitution for Glutamate, Aspartate, Leucine, Valine and Asparagines (Fig. 2).

250 The phylogenetic analysis depicts the evolutionary relatedness of the ToxA1 amino
251 acid sequence with other ToxA sequences. The tree indicates that ToxA sequences originate
252 from a common ancestor but form different clades during evolution. The ToxA sequence from
253 all the *Bipolaris* isolates formed an independent clade along with *Py. tritici-repentis* and
254 diverged from *P. nodorum*. This indicates sequence similarity among *B. sorokiniana* and *Py.*
255 *tritici-repentis,* whereas it differed from *P. nodorum* (Fig. 3).

256 ***Protein modelling and Topographical properties***

257 The structure of the ToxA1 protein of a cloned gene of *B. sorokiniana* isolate MCC1533
258 (Pusa2) was predicted using the SWISS-MODEL homology modelling online server. For
259 checking the reliability of models GMQE (ToxA1: 0.56), QMEAN Z scores are included
260 QMEAN -0.33, Cbeta –1.79, torsion 0.53 and these scores indicated that these models are
261 reliable and good quality. The quality of the resulting models was monitored with
262 PROCHECK. Ramachandran plot analysis revealed that 88.1% of the ToxA1 protein structure
263 residues fell within the most favoured regions, with a further 11.9% in the additionally allowed
264 region (Fig. 4). No residues were found in the generously allowed or disallowed regions. The
265 number of non-glycine and non-proline residues was 100%. The number of end residues
266 (excluding Gly and Pro) is 2, and the number of glycine and proline residues was 12 and 3,
267 respectively.

268 Predicted ToxA1 protein structures of *B. sorokiniana* MCC1533 (Pusa2) isolate based
269 on homology modelling are depicted in Fig. 4. The protein sequences of ToxA1 protein showed
270 sequence identity of 100% with template PDB entry 1zld.1.A (*Py. tritici-repentis*, *PtrToxA*).

271 When generated structures were compared in UCSF Chimera, it was observed that the RGD
272 motif (Toxic region) was present in the 3D structure of ToxA1 protein and found that arginine
273 is present in the alpha helix of the loop at 118 positions. At the same time, Glycine and Aspartic
274 acid is present in the β-sheet of the protein structure at 119 and 120 positions of ToxA1 protein
275 (Fig. 5). The percentage of the alpha helix was 3.39%. At the same time, antiparallel sheet 1
276 was 35.55%, antiparallel sheet 2 was 12.76%, the parallel sheet was 0.85%, the turn was 7.63%,
277 and the other was 39.83%.

278 ***Bioactivity of ToxA1 effector protein and its interaction with Tsn1 at both seedling and adult***
279 ***stage***

280 The bioactivity of the *ToxA1* effector was studied on necrotic lesions symptoms caused due to
281 *ToxA1* protein and was found to be more prominent at the adult stage. At the seedling stage,
282 the maximum area (0.977 cm^2) was recorded in genotype K68(*Tsn1*) and the minimum 0.265
283 cm^2 in WAMI280 (*tsn1*). At the same time, the length varies from 2.872 cm (K68, *Tsn1*) to
284 0.860cm (PBW343, *tsn1*). However, the maximum width recorded was 0.432 cm for genotype
285 WAMI288 (*Tsn1*), and the minimum in genotype harbouring *tsn1*(LOK1) was 0.307cm.
286 At the adult stage, the length of the symptom was maximum (4.613cm) in genotypes
287 harbouring*Tsn1*(K68) and minimum (1.305 cm) WAMI280 (*tsn1*), and the width also showed
288 the same trend varies from 0.633cm (C306, *Tsn1*) to 0.327cm (WAMI280, *tsn1*). The area was
289 measured for quantifying the necrotrophic symptom, and it found that the maximum area in
290 the genotype harboring *Tsn1* was 2.326 cm^2 (K68), and the minimum was 0.411
291 cm^2(WAMI280, *tsn1*). A significant difference was found between the seedling and adult
292 stages and for *Tsn1* and *tsn1* (Table 1, Fig. S2, S3, S4).

293 **Discussion**

294 Studies on necrotrophic effectors producing HSTs have provided a new dimension to host-
295 pathogen interaction and established an inverse gene-for-gene relationship (Friesen et al. 2006,

296 Navathe et al. 2020). The HSTs are effectors proteins and induce a susceptible response in the
297 host harbouring the dominant susceptibility gene. ToxA is a necrotrophic effector protein, one
298 of the key factors for causing the most devastating disease, spot blotch in wheat, prevalent in
299 warm, humid regions of South Asia. The present study focuses on cloning of *ToxA1* gene,
300 followed by its characterization and purification of the resultant protein and its expression
301 analysis. In this study, we have successfully cloned and characterized the *ToxA1* gene from *B.*
302 *sorokiniana* isolate MCC1533 (Pusa2). This gene was originally found in *P. nodorum* and
303 horizontally transferred to *Py. tritici-repentis* and, more recently, to *B. sorokiniana* (Friesen et
304 al. 2006, McDonald et al. 2012) . The cloned gene and its expression were studied in the present
305 study, and the purified protein showed peak expression at a concentration of 1.0 mM IPTG
306 with band migration at 16.5kDa in size. Manning et al. (2008) also reported similar findings
307 where lysates with His-ToxA1 or without (control) have a phosphorylated band that migrates
308 at 16 kDa. However, Mass spectral analyses have indicated a 13.2 kDa mass of purified mature
309 ToxA1 protein from *Py. tritici-repentis* (Ciuffetti et al. 1997, Tuori et al. 1995). The importance
310 of a protein purification study for ToxA1, which has selective host toxicity for genetic analysis
311 of pathogenicity in the *Pyrenophora*-wheat interaction, was also suggested by Touri et al.
312 (1995).
313 The *ToxA1* gene was truncated in the present study to remove the signalling sequences, which
314 comprise 22 amino acids, as the mature ToxA1 gene is released after the proteolytic cleavage
315 of this signal sequence. Previous studies have also described these signalling peptides in ToxA
316 protein that involve the first 22 amino acids, which are proteolytically cleaved after import into
317 the endomembrane system (Ciuffetti et al. 1997). The release of mature toxin involves
318 additional proteolytic processing, and as the ToxA1 protein is blocked at the N terminus, such
319 modifications would incur a mass increase (Ciuffetti et al. 1997). The ToxA1 cloned sequence
320 obtained in our study has been compared with the already reported ToxA1 sequences from *P.*

321 *nodorum*, *Py. tritici-repentis* and *B. sorokiniana*. Multiple sequence alignment of amino acid
322 sequences from 26 isolates was performed. The results suggest that the ToxA region from *B.*
323 *sorokiniana* and *Py. tritici-repentis* show evolutionary origin relatedness to each other than to
324 *P. nodorum*. This is based on the identical ToxA1 sequence shared between *B. sorokiniana* and
325 *Py. tritici-repentis* and the difference at six positions in *P. nodorum* haplotypes (Fig. 2). The
326 sequence identity between the three fungal species accounts for the common evolutionary
327 origin of ToxA and the potential of exchanging DNA between these species (McDonald et al.
328 2018). The significance of phylogenetic studies in establishing evolutionary relationships
329 among the different pathogen races or deriving the specific gene evolution between different
330 genera is well known. The sequencing data for ToxA1 showed a high degree of similarity
331 between *B. sorokiniana* and *Py. tritici-repentis* (Hafez et al. 2022, Aboukhaddour et al. 2023).
332 Previous studies have also suggested that the ToxA1 sequence did not differ for *B. sorokiniana*
333 and *Py. tritici-repentis* but differed from the ToxA sequence of *P. nodorum* (Navathe et al.
334 2020, Hafez et al. 2022, Aboukhaddour et al. 2023). This evolutionary relatedness of *Py. tritici-*
335 *repentis* and *B. sorokiniana* sequences have also been reported earlier (McDonald et al. 2018,
336 Navathe et al. 2020). The earlier report suggested that ToxA has been present in *P. nodorum*
337 for a long time as it exhibited greater sequence diversity and was interspecifically transferred
338 to *Py. tritici-repentis* quite later. This is evident from monomorphism or lesser sequence
339 diversity in the ToxA1 sequence from *Py. tritici-repentis* and the emergence of tan spot
340 symptoms more recently in the near past (Aboukhaddour et al. 2023).
341 Further insights into the ToxA structural analysis were performed by predicting the 3D protein
342 structure using an amino acid sequence of ToxA1 (Fig.4). This is the first report for the 3D
343 protein structure ToxA1 haplotype from *B. sorokiniana*. The predicted protein structure was
344 similar to a single-domain protein with a β-sandwich fold of PtrToxA. This β-fold represents a
345 solvent-exposed loop containing arginyl-glycol-aspartic acid (RGD)- functionally active motif

346 [(Sarma et al 2005, Ciuffetti et al. 2010). ToxA1 has been known to resemble with fibronectin
347 III domain which retains a solvent-exposed loop containing RGD motif for cell wall-plasma
348 membrane interaction in plants (Ciuffetti et al. 2010, McDonald and Solomon 2018). It has
349 been proposed that ToxA with RGD-containing motif has been known to interact with wheat
350 mesophyll cells and thus establish disease (Manning et al. 2007) The mesophyll cells have a
351 high-affinity matrix to recognise these motifs, and these all suggest the importance of the RGD
352 motif in receptor binding and internalisation into wheat cells (Ciuffetti et al. 2010).
353 ToxA is the only known virulence gene for which a host sensitivity gene (*Tsn1*) has been known
354 in wheat-*B. sorokiniana* pathosystem. For the first time, the present study reports a cloned and
355 purified protein ToxA1 infiltration in both seedling and adult stages of wheat lines harbouring
356 *Tsn1/tsn1*. The severity was found to be enhanced in the adult stage compared to the seedling
357 stage in *Tsn1* wheat lines. The present data also reveals that *Tsn1*-carrying genotypes exhibited
358 more disease in seedlings than in the adult stage. The toxin activity was highest in the K68
359 genotype (*Tsn1*) and lowest in WAMI280 (*tsn1*) at both the seedling and adult stages. This
360 could be validated by past studies where it has been suggested that ToxA causes severe necrotic
361 lesions on *Tsn1,* harbouring wheat genotypes, while less or no lesion was observed for wheat
362 genotypes lacking the sensitivity gene (Aggarwal et al 2021). Navathe et al. (2020) also
363 reported one such possibility of the involvement of a recessive allele of *Sb2* towards an
364 unknown HST. *Tsn1* has been reported attributing susceptibility towards both *P. nodorum*-
365 causing SNB (Friesen et al 2006, Virdi et al. 2016) and *Py. tritici-repentis* are causing tan spots
366 (Faris et al. 2013). However, the environmental requirements for *Bipolaris* are different from
367 these two pathogens, which are not found in the South-Asian region.
368 Nevertheless, it would be desirable for wheat breeders to select *tsn1* for making crops resistant
369 to these three pathogens. The study in this horizon should focus on the presence of loci other

than *Tsn1* and *Sb2*. It would be interesting to study other quantitative trait loci involved to understand the complexity of this *ToxA-Tsn1* interaction.

Acknowledgements: Authors acknowledge Banaras Hindu University and Bihar Agricultural University for the infrastructure facility
Funding: SN acknowledges SERB, New Delhi, for CRG/2021/007211.

Author Contributions: Conceptualization, RC, VKM, PKS, SN, and SK; methodology, RKC and DT; validation, DT and SKS; formal analysis DT and SKS; investigation, RKC; resources, RC, DT; data curation, DT, SKS; writing—original draft preparation, RKC, SN; writing—review and editing, RC, PKS; supervision, RC, VKM, SKS; project administration, RC; funding acquisition, RC, PKS. All authors have read and agreed to the published version of the manuscript.

Availability of data and materials: Not applicable.

Declarations

Ethics approval and consent to participate: Not applicable.

Consent for publication: Not applicable.

Competing interests: The authors declare that they have no competing interests.

Ciuffetti, L. M., Tuori, R. P. Gaventa, J. M. A single gene encodes a selective toxin causal to the development of tan spot of wheat. Plant Cell, 1997, *9*, 135-144. https://doi.org/10.1105/tpc.9.2.135

Wolpert, T.J., Dunkle, L.D., Ciuffetti, L.M. Host-selective toxins and avirulence determinants: what's in a name? Annu. Rev. Phytopathol. 2002, 40, 251–285. https://doi.org/10.1146/annurev.phyto.40.011402.114210

Sharma, P., Duveiller, E., Sharma, R. C. Effect of mineral nutrients on spot blotch severity in wheat and associated increases in grain yield. Field Crops Res, 2006, *95*, 426-430. https://doi.org/10.1016/j.fcr.2005.04.015

Pandey AK, Mishra VK, Chand R, Navathe S, Budhlakoti N, Srinivasa J, Sharma S, Joshi AK. Crosses with spelt improve tolerance of South Asian spring wheat to spot blotch, terminal heat stress, and their combination. Sci Rep, 2021, *11*, 1-12. https://doi.org/10.1038/s41598-021-85238-x

Ballance, G.M., Lamari, L., Bernier, C.C. Purification and characterization of a host-selective necrosis toxin from Pyrenophora tritici-repentis. Physiol. Mol. Plant Pathol. 1989, *35*, 203–213 https://doi.org/10.1016/0885-5765(89)90051-9

Friesen, T. L., Stukenbrock, E. H., Liu, Z., Meinhardt, S., Ling, H., Faris, J. D., ... Oliver, R. P. Emergence of a new disease as a result of interspecific virulence gene transfer. Nat. Genet. 2006, *38*: 953-956. https://doi.org/10.1038/ng1839

McDonald, M. C., & Solomon, P. S. Just the surface: advances in the discovery and characterization of necrotrophic wheat effectors. Curr. Opin. Microbiol. 2018, *46*, 14-18.

Solomon, P., Lowe, R., Tan, K.C., Waters, O., Oliver, R. *Stagonospora nodorum*; cause of Stagonospora nodorum blotch of wheat. Mol. Plant Pathol. 2006, *7*, 147–156 https://doi.org/10.1111/j.1364-3703.2006.00326.x

412 Tuori, R. P., Wolpert, T. J. Ciuffetti, L. M. Purification and immunological characterization
413 of toxic components from cultures of *Pyrenophora tritici-repentis*. Mol. Plant Microbe
414 Interact, 1995, *8*, 41-48. https://doi.org/10.1094/mpmi-8-0041
415 Tomás, A., Bockus, W. W. Cultivar specific toxicity of culture filtrate of *Pyrenophora tritici-*
416 *repentis*. Phytopathology, 1987, *77*,1337–1366. https://doi.org/10.1094/phyto-77-1337
417 McDonald, M. C., Ahren, D., Simpfendorfer, S., Milgate, A. Solomon, P. S. The discovery of
418 the virulence gene ToxA in the wheat and barley pathogen *Bipolaris sorokiniana*. Mol.
419 Plant Pathol., 2018, *19*, 432-439. https://doi.org/10.1111/mpp.12535
420 Ballance, G. M., Lamari, L., Kowatsch, R., Bernier, C. C. Cloning, expression and occurrence
421 of the gene encoding the Ptrnecrosistoxin from *Pyrenophora tritici-repentis*. Mol. Plant
422 Pathol. 1996, https://doi.org/10.1007/978-94-011-5218-1_21
423 Tuori, R. P., Wolpert, T. J. Ciuffetti, L. M. Heterologous expression of functional PtrToxA.
424 Mol. Plant Microbe Interact, 2000, *13*, 456-464.
425 https://doi.org/10.1094/mpmi.2000.13.4.456.
426 Faris, J. D., Zhang, Z., Lu, H., Lu, S., Reddy, L., Cloutier, S., ... Friesen, T. L. A unique wheat
427 disease resistance-like gene governs effector-triggered susceptibility to necrotrophic
428 pathogens. PNAS, 2010, *107*, 13544-13549. https://doi.org/10.1073/pnas.1004090107
429 Lamari, L., Bernier, C. C. Evaluation of wheat lines and cultivars to tan spot [*Pyrenophora*
430 *tritici-repentis*] based on lesion type. Comput. Appl. Biosci. 1989, 11, 49-56.
431 https://doi.org/10.1080/07060668909501146
432 Tan, K. C., Ferguson-Hunt, M., Rybak, K., Waters, O. D., Stanley, W. A., Bond, C. S.,
433 Stukenbrock, E. H., Friesen, T. L., Faris, J. D., McDonald, B. A., Oliver, R. P.
434 Quantitative variation in effector activity of ToxA isoforms from *Stagonospora nodorum*
435 and *Pyrenophora tritici-repentis*. Mol. Plant Microbe Interact. 2012, *25*, 515-522.
436 https://doi.org/10.1094/mpmi-10-11-0273
437 Sambrook, J., Russell, D. W., Sambrook, J. The condensed protocols: from molecular cloning:
438 a laboratory manual, 2006, (No. Sirsi) i9780879697723). Cold Spring Harbor, NY: Cold
439 spring harbour laboratory press. https://doi.org/10.1101/pdb.prot4018
440 Hall, T. A. A user-friendly Biological Sequence Alignment Editor and Analysis program for
441 Windows 95/98/NT. Nucleic Acids Symp Ser, 1999, *41*, 95–98
442 Altschul S. F., Madden T.L., Schäffer A.A., Zhang J., Zhang Z., Miller W., Lipman D. J.
443 Gapped BLAST and PSI-BLAST: a new generation of protein database search programs.
444 Nucleic Acids Res. 1997, *25*, 3389–3402. https://doi.org/10.1093/nar/25.17.3389
445 Kumar S., Stecher G., Li M., Knyaz C., Tamura K. MEGA X: MolecularEvolutionary Genetics
446 Analysis across computing platforms. Mol Biol Evol. 2018, *35*, 1547–1549.
447 https://doi.org/10.1093/molbev/msy096
448 Larkin M.A., Blackshields G., Brown N.P., Chenna R., McGettigan P.A., McWilliam H.,
449 Valentin F., Wallace I.M., Wilm A., Lopez R., Thompson J.D. Clustal W and Clustal X
450 version 2.0. Bioinformatics, 2007, *23*, 2947–2948.
451 https://doi.org/10.1093/bioinformatics/btm404
452 Jones DT, Taylor WR, Thornton JM. The rapid generation of mutation data matrices from
453 protein sequences. Comput. Appl. Biosci. 1992, *8*, 275-282.
454 https://doi.org/10.1093/bioinformatics/8.3.275

455 Felsenstein. Confidence limits on phylogenies: an approach using the bootstrap. Evolution
456 1985, *39*, 783–791. https://doi.org/10.1111/j.1558-5646.1985.tb00420.x
457 Arnold K, Bordoli L, Kopp J, Schwede T. The SWISS-MODELworkspace: a web-based
458 environment for protein structure homology modelling. Bioinformatics 2006, *22*, 95–
459 201. https://doi.org/10.1093/bioinformatics/bti770
460 Benkert P, Tosatto SCE, Schwede T. Global and local model quality estimation at CASP8
461 using the scoring functions QMEAN and QMEANclust. Proteins Struct Funct
462 Bioinforma. 2009, *77*, 173–180. https://doi.org/10.1002/prot.22532
463 Studer G, Rempfer C, Waterhouse AM, Gumienny R, Haas J, Schwede T. QMEAND is Co—
464 distance constraints applied on model quality estimation. Bioinformatics, 2020, *36*,1765–
465 1771. https://doi.org/10.1093/bioinformatics/btz828
466 Laskowski RA, MacArthur MW, Moss DS, Thornton JM. PROCHECK: a program to check
467 the stereochemical quality of protein structures. J. Appl. Crystallogr. 1993, 26, 283–291
468 https://doi.org/10.1107/s0021889892009944
469 Tian W, Chen C, Lei X, Zhao J, Liang J. CASTp 3.0: computed atlas of surface topography of
470 proteins. Nucleic Acids Res. 2018, *46*, W363–W367. https://doi.org/10.1093/nar/gky473
471 Pettersen EF, Goddard TD, Huang CC, Couch GS, Greenblatt DM, Meng EC, Ferrin TE. UCSF
472 Chimera. A visualization system for exploratory research and analysis. J Comput Chem.
473 2004, *25*, 1605–1612 https://doi.org/10.1002/jcc.20084
474 R Core Team. R: A language and environment for statistical computing. 2022, R Foundation
475 for Statistical Computing, Vienna, Austria. https://www.R-project.org/.
476 Navathe S, Yadav PS, Chand R, Mishra VK, Vasistha NK, Meher PK, Joshi AK, Gupta PK.
477 ToxA–Tsn1 interaction for spot blotch susceptibility in Indian wheat: An example of
478 inverse gene-for-gene relationship. Plant dis, 2020, *104,* 71-81.
479 https://doi.org/10.1094/pdis-05-19-1066-re
480 McDonald, M.C., Razavi, M., Friesen, T.L., Brunner, P.C., McDonald, B.A. Phylogenetic and
481 population genetic analyses of *Phaeosphaeria nodorum* and its close relatives indicate
482 cryptic species and an origin in the Fertile Crescent. Fungal Genet. Biol. 2012, *49*, 882–
483 895. https://doi.org/10.1016/j.fgb.2012.08.001
484 Manning, V. A., Hamilton, S. M., Karplus, P. A., Ciuffetti, L. M. The Arg-Gly-Asp–
485 containing, solvent-exposed loop of PtrToxA is required for internalization. Mol. Plant
486 Microbe Interact. 2008, *21*, 315-325. https://doi.org/10.1094/mpmi-21-3-0315
487 McDonald, M. C., Solomon, P. S. Just the surface: advances in the discovery and
488 characterization of necrotrophic wheat effectors. Curr. Opin. Microbiol. 2018, 46, 14-18.
489 Hafez, M., Despins, T., Nakajima, K., Aboukhaddour, R. Identification of a novel ToxA
490 haplotype of *Pyrenophora tritici-repentis* from Japan. Phytopathology, 2022, *112*, 1597-
491 1602 https://doi.org/10.1094/phyto-01-22-0001-sc
492 Aboukhaddour, R., Abdel-Fattah, M. H., McDonald, M., Moffat, C., Navathe, S., Friesen, T.
493 L., Strelkov, S. E., Oliver, R. P., Tan, K.-C., Liu, Z., Moolhuijzen, P., Phan, H., See, P.
494 T., Solomon, P. A revised nomenclature for ToxA haplotypes across multiple fungal
495 species. Phytopathology, 2023, https://doi.org/10.1094/phyto-01-23-0017-sc
496 Sarma GN, Manning VA, Ciuffetti LM, Karplus PA. Structure of PtrToxA: an RGD-containing
497 host-selective toxin from *Pyrenophora tritici-repentis*. Plant Cell, 2005, *17*, 3190–3202.
498 https://doi.org/10.1105/tpc.105.034918

499 Ciuffetti, L. M., Manning, V. A., Pandelova, I., Betts, M. F., Martinez, J. P. Host‐selective
500 toxins, PtrToxA and PtrToxB, as necrotrophic effectors in the *Pyrenophora tritici‐*
501 *repentis*‐wheat interaction. New Phytol. 2010, *187*, 911-919.
502 https://doi.org/10.1111/j.1469-8137.2010.03362.x
503 Baluska, F., Samaj, J., Wojtaszek, P., Volkmann, D., Menzel, D. Cytoskeleton-plasma
504 membrane-cell wall continuum in plants. Emerging links revisited. Plant Physiol. 2003,
505 *133*, 482-491. https://doi.org/10.1104/pp.103.027250
506 Manning, V. A., Hardison, L. K., Ciuffetti, L. M. PtrToxA interacts with a chloroplast-
507 localized protein. Mol. Plant Microbe Interact. 2007, *20*, 168-177.
508 https://doi.org/10.1094/mpmi-20-2-0168
509 Aggarwal, R., Agarwal, S., Sharma, S., Gurjar, M. S., Bashyal, B. M., Rao, A. R., Saharan, M.
510 S. Whole Genome Sequencing and Expression Analysis of ToxA in *Bipolaris*
511 *sorokiniana* Provides Discernment of Pathogenicity Causing Spot Blotch of Wheat.
512 2021, PREPRINT (Version 1) available at Research Square.
513 https://doi.org/10.21203/rs.3.rs-677095/v1
514 Virdi, S., Liu, Z., Overlander, M., Zhang, Z., Xu, S. S., Friesen, T., Faris, J. D. New insights
515 into the roles of host gene-necrotrophic effector interactions in governing susceptibility
516 of durum wheat to tan spot and Septoria nodorum blotch. Genes Genomes Genet. 2016,
517 *6*, 4139-4150. https://doi.org/10.1534/g3.116.036525
518 Faris, J. D., Liu, Z. Xu, S. S. Genetics of tan spot resistance in wheat. Theor. Appl. Genet.,
519 2013, *126*, 2197-2217. https://doi.org/10.1007/s00122-013-2157-y

520

521 **Figure Legends**

522 **Figure 1**. Expressed ToxA1 protein showing 16.5kd band size on SDS-PAGE
523 **Figure 2** (a.) The multiple sequence alignments with a phylogenetic tree, Colors both on the
524 phylogenetic tree and on the branch, scale represent genetic distance. ToxA sequences
525 have been colored by four different colors shown in the 'seq' column for each
526 nucleotide. Color changes on the aligned sequences represent nucleotide differences.
527 (b) Heat map based on the number of nucleotide differences between the ToxA
528 haplotypes. Each branch of the phylogenetic tree represents the corresponding ToxA
529 haplotype in the matrix. The close relationships with "darkred" color and far
530 relationships with "white" color. (c) Neighbor-joining (NJ) tree for ToxA haplotypes of
531 based on the nucleotide sequence differences. Colored internal nodes represent the
532 bootstrap confidence level.
533 **Figure 3** Phylogenetic tree using Maximum Likelihood algorithm of different ToxA1 of
534 *Pyrenophora tritici-repentis, Bipolaris sorokiniana,* and varipus haplotypes of
535 *Parastagnospora nodorum*. The percentage of bootstrap support (1000 replicates) is
536 indicated at corresponding nodes. The nomenclature of the haplotypes is based on the
537 Aboukhaddour et al. (2023)

538 **Figure 4.** Ramachandran plot and ProsSA z-score analysis of modelled ToxA1 protein from
539 *B. sorokiniana*. Ramachandran distributions of amino acids in the model were
540 calculated using pro check (a), and the z-score plot was plotted using ProsSA-WEB (b).
541 **Figure 5.** *ToxA1* protein structure of *B. sorokiniana* isolate MCC 1533 (Pusa2) depicting
542 conserved RGD motif (ARG-GLY-ASP)
543 **Figure 6.** Symptom on *Tsn1/tsn1* harboring genotypes after infiltration ToxA1 protein at
544 seedling and adult plant stage.

545 **Table Legends**

546 **Table1.** Symptom of spot blotch after infiltration of *ToxA1* protein at both seedling and adult
547 stage of wheat genotypes harboring *Tsn1/tsn1* allele.

548 **Supplementary Materials:**

549 **Figure S1.** Correlation matrix of phenotypic traits Tsn1/tsn1 gene effect on inoculation with
550 ToxA1 isolate**;**
551 **Figure S2.** Necrotrophic area developed due to ToxA1–Tsn1 interaction at both seedling and
552 adult stage of wheat genotypes**;**
553 **Figure S3**. Symptom of spot blotch after infiltration ToxA1 protein at both seedling and adult
554 stage of wheat genotypes harbouring *Tsn1*;
555 **Figure S4**. Symptom of spot blotch after infiltration ToxA1 protein at both seedling and adult
556 stage of wheat genotypes harbouring *tsn1*
557

Table1: Symptom of spot blotch after infiltration of *ToxA1* protein at both seedling and adult stage of wheat genotypes harboring *Tsn1/tsn1* allele

Genotypes	**Length(cm)**		**Width(cm)**		**Area(cm2)**		**Tsn1/tsn1**
	Seedling	Adult	Seedling	Adult	Seedling	Adult	
K 68	2.872	4.613	0.404	0.530	0.977	2.326	*Tsn1*
C 306	1.921	4.226	0.329	0.633	0.678	1.737	*Tsn1*
HUW468	2.057	3.472	0.402	0.438	0.718	1.407	*Tsn1*
Yangmai 6	0.860	1.406	0.311	0.381	0.316	0.450	*Tsn1*
K65	1.513	2.582	0.380	0.566	0.388	1.096	*Tsn1*
WAMI160	1.615	3.461	0.345	0.506	0.646	1.521	*Tsn1*
WAMI188	1.693	2.582	0.310	0.500	0.585	1.036	*Tsn1*
WAMI224	1.643	2.857	0.330	0.488	0.476	1.298	*Tsn1*
WAMI226	1.782	2.320	0.405	0.503	0.628	1.090	*Tsn1*
WAMI277	1.464	2.174	0.360	0.485	0.464	1.024	*Tsn1*
WAMI288	1.591	2.054	0.432	0.575	0.622	1.017	*Tsn1*
Max.	2.872	4.613	0.432	0.633	0.977	2.326	
Min.	0.860	1.406	0.310	0.381	0.316	0.450	
HUW234	0.964	1.894	0.335	0.408	0.345	0.561	*tsn1*
PBW343	0.860	1.446	0.349	0.408	0.319	0.423	*tsn1*
LOK1	1.098	1.761	0.307	0.432	0.278	0.493	*tsn1*
Sonalika	1.919	2.923	0.361	0.492	0.584	1.321	*tsn1*
WAMI280	0.972	1.305	0.319	0.327	0.265	0.411	*tsn1*
WAMI289	1.065	1.471	0.319	0.344	0.342	0.529	*tsn1*
WAMI290	1.206	1.467	0.327	0.360	0.365	0.493	*tsn1*
Max.	1.919	2.923	0.361	0.492	0.584	1.321	
Min.	0.860	1.305	0.307	0.327	0.265	0.411	

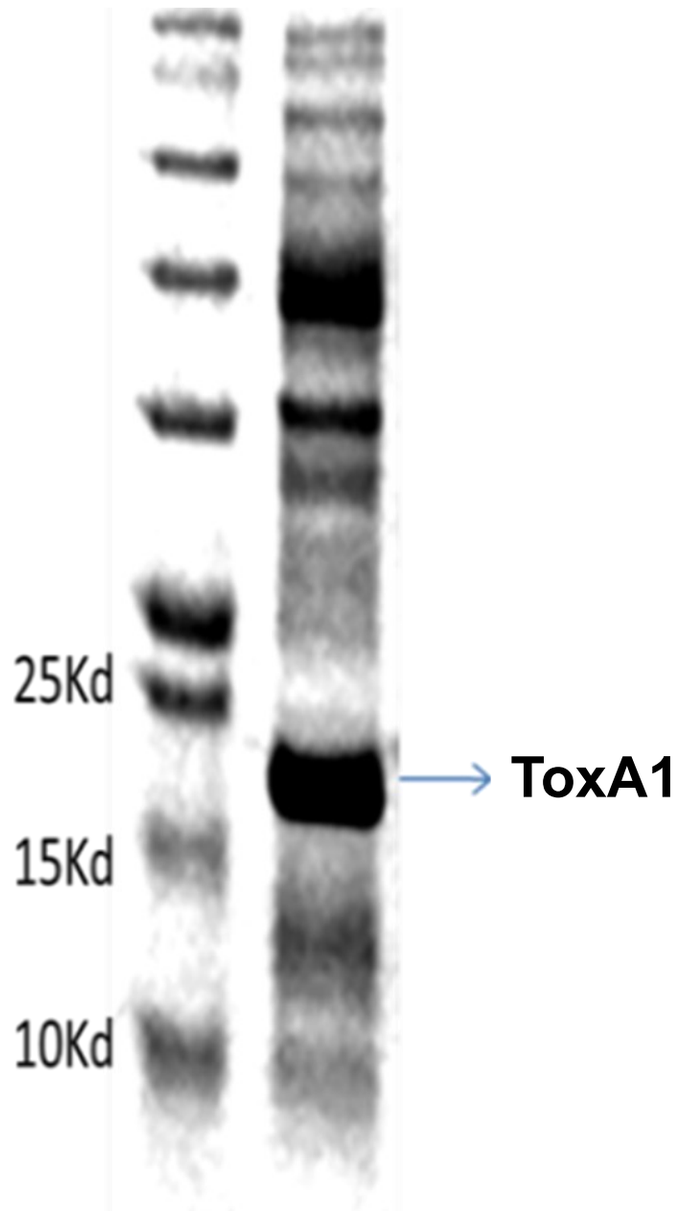

Fig.1: Expressed ToxA1 protein showing 16.5kd band size on SDS-PAGE

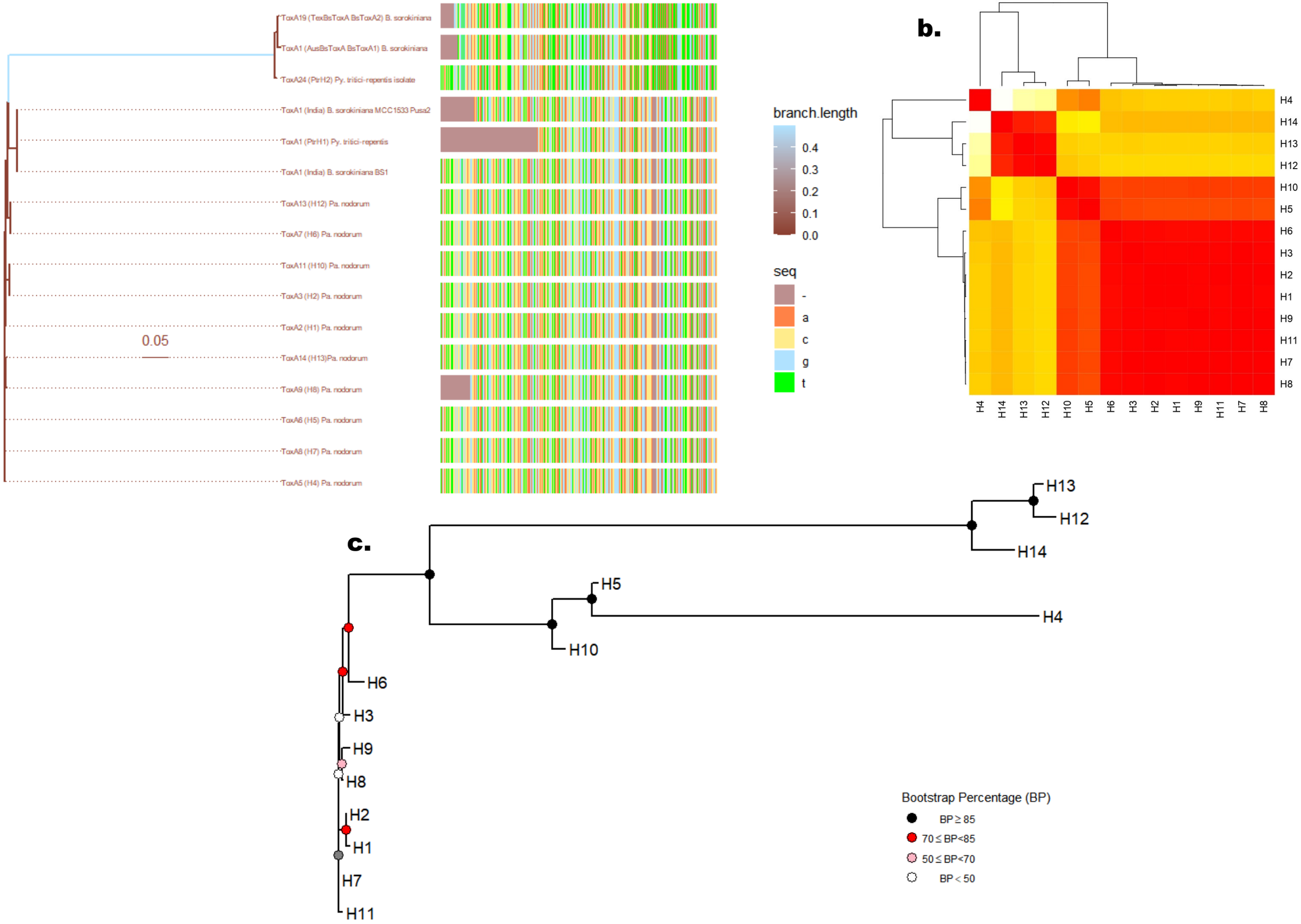

Fig2 (a.) The multiple sequence alignments with a phylogenetic tree, Colors both on the phylogenetic tree and on the branch scale represent genetic distance. *ToxA* sequences have been colored by four different colors shown in the 'seq' column for each nucleotide. Color changes on the aligned sequences represent nucleotide differences. **(b) Heat map based on the number of nucleotide differences between the ToxA haplotypes.** Each branch of the phylogenetic tree represents the corresponding ToxA haplotype in the matrix. The close relationships with "darkred" color and far relationships with "white" color. **(c) Neighbor-joining (NJ) tree for ToxA haplotypes of based on the nucleotide sequence differences.** Colored internal nodes represent the bootstrap confidence level.

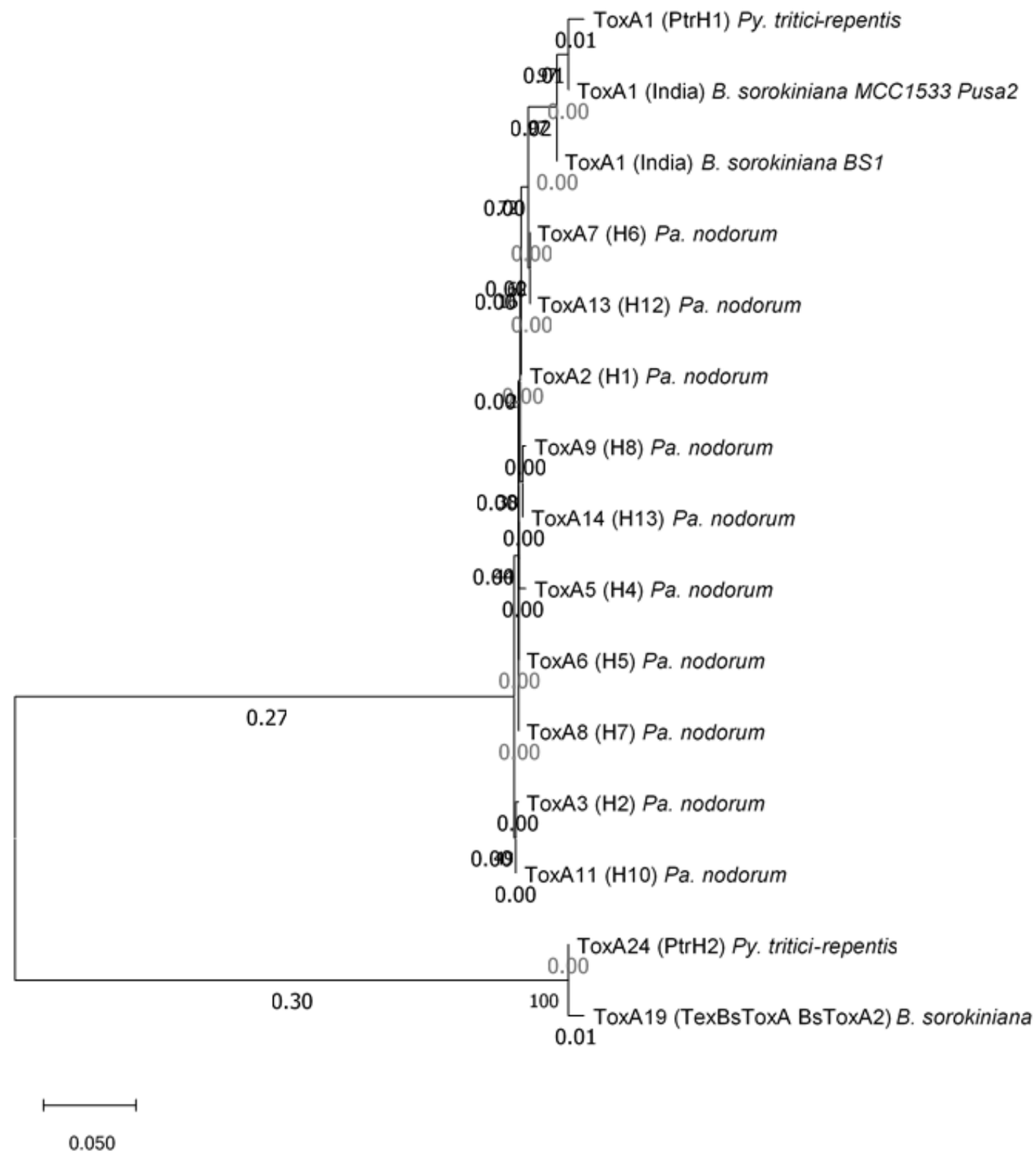

Fig. 3: Phylogenetic tree using Maximum Likelihood algorithm of different ToxA1 of *Pyrenophora tritici-repentis, Bipolaris sorokiniana,* and varipus haplotypes of *Parastagnospora nodorum*. The percentage of bootstrap support (1000 replicates) is indicated at corresponding nodes. The nomenclature of the haplotypes is based on the Aboukhaddour et al. (2023)

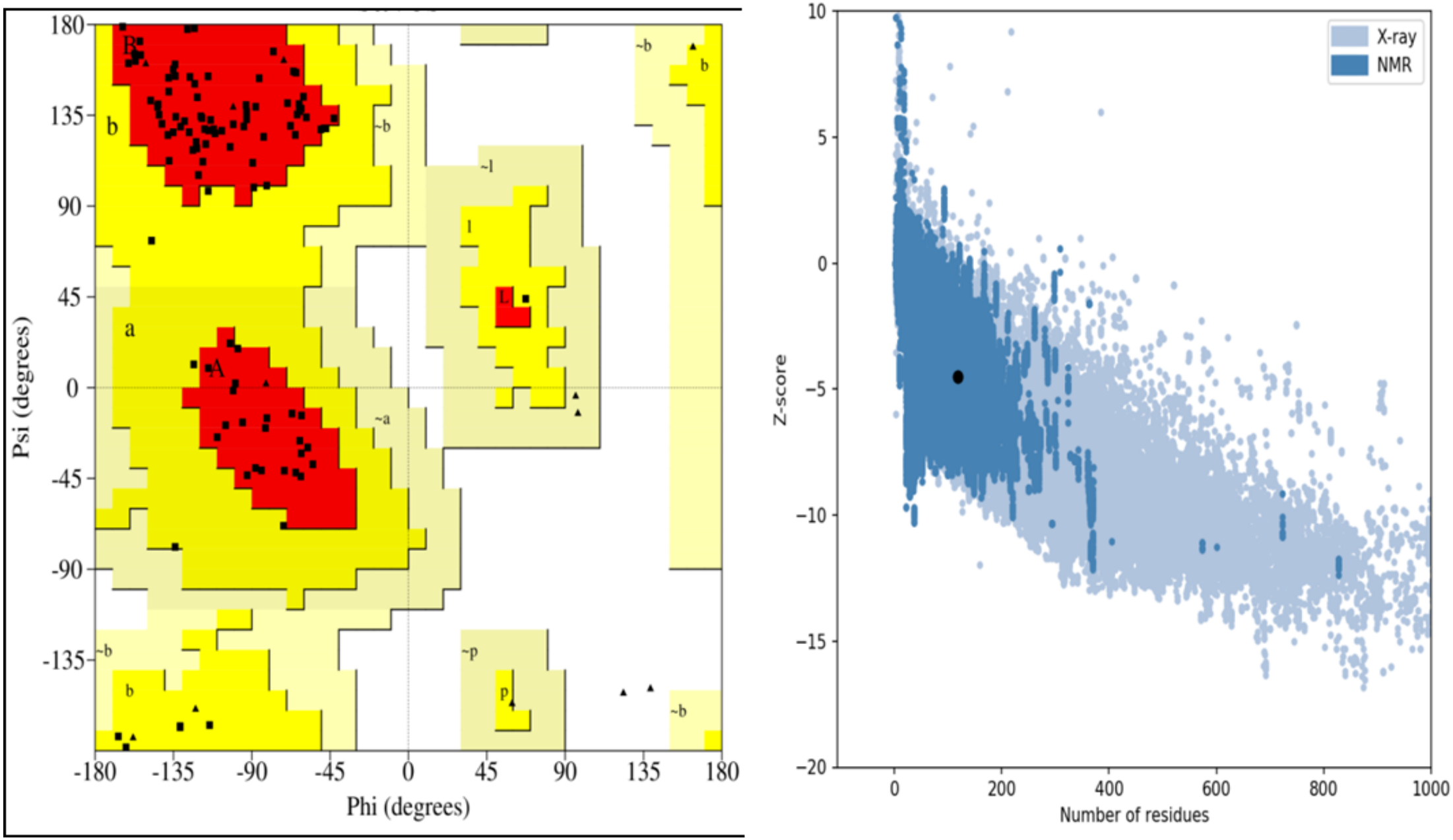

Fig. 4: Ramachandran plot and ProsSA z-score analysis of modelled ToxA1 protein from *B. sorokiniana*. Ramachandran distributions of amino acids in the model were calculated using pro check (a), and the z-score plot was plotted using ProsSA-WEB (b).

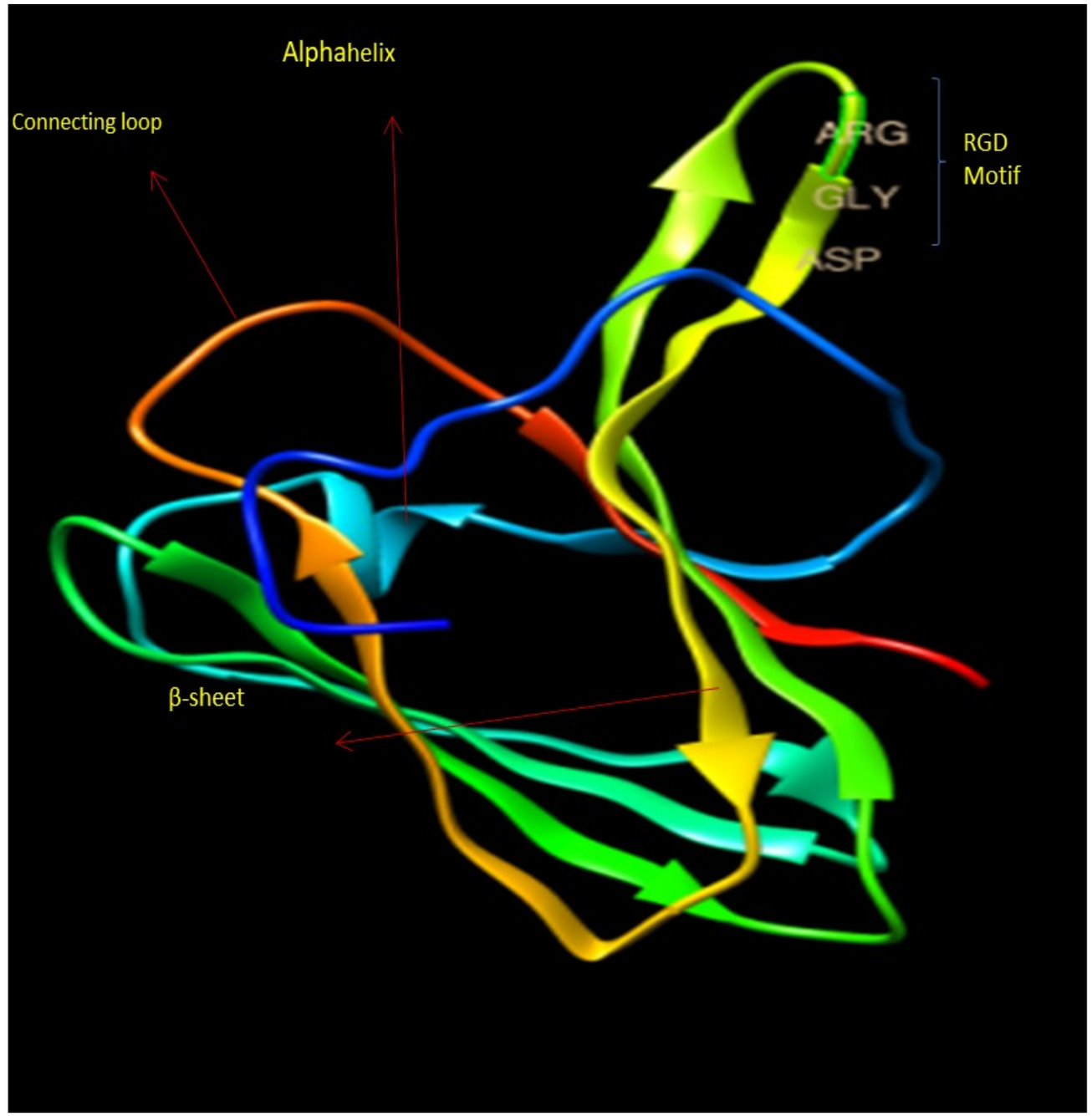

Fig. 5: *ToxA1* protein structure of *B. sorokiniana* isolate MCC 1533 (Pusa2) depicting conserved RGD motif (ARG-GLY-ASP)

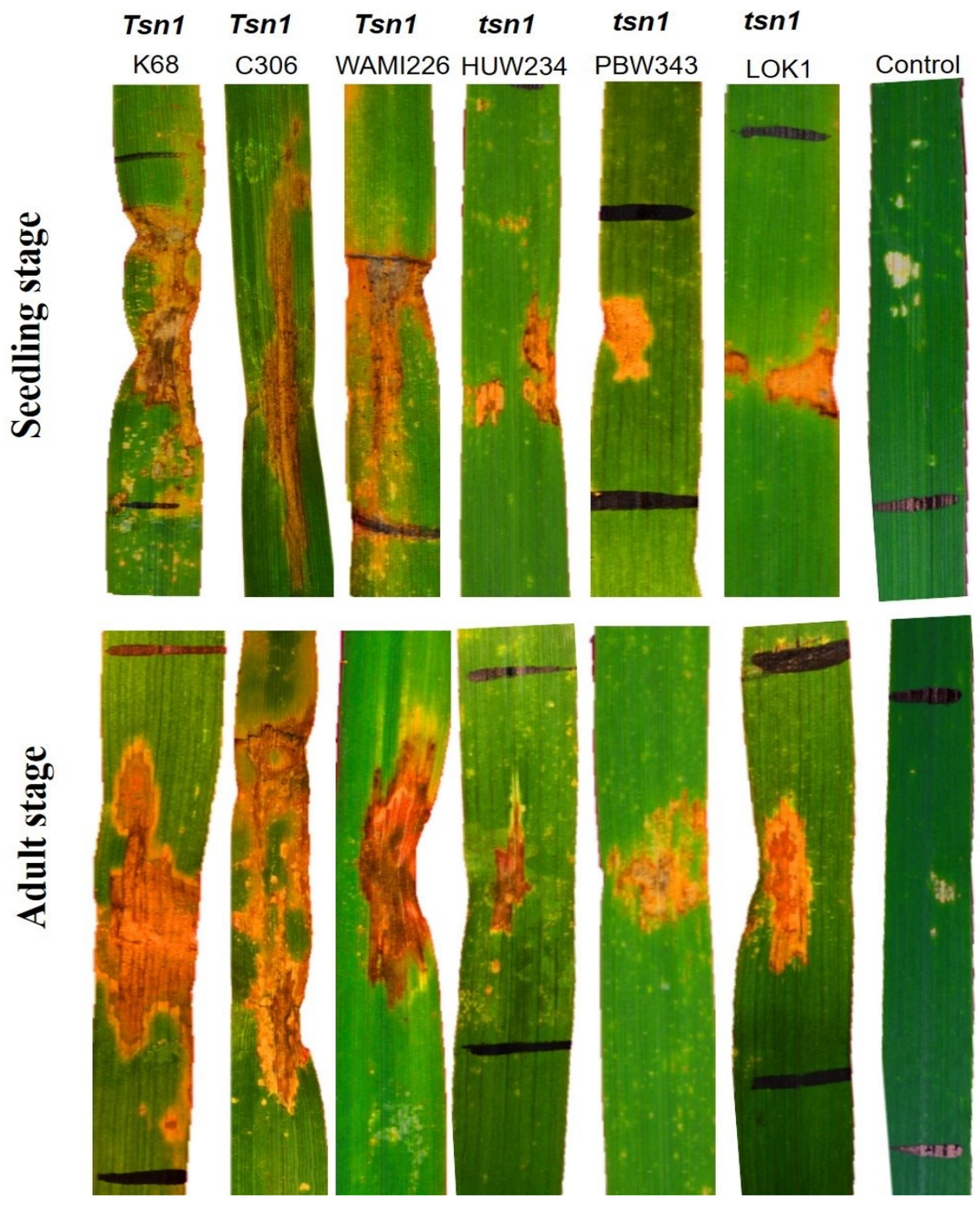

Fig. 6 Symptom on *Tsn1/tsn1* harboring genotypes after infiltration ToxA1 protein at seedling and adult plant stage.